Quantum Electronics **51** (8) 679–682 (2021)

https://doi.org/10.1070/QEL17596

Laser amplification in an Yb:YAG active mirror with a significant temperature gradient

G.V. Kuptsov, V.A. Petrov, V.V. Petrov, A.V. Laptev, A.O. Konovalova, A.V. Kirpichnikov, E.V. Pestryakov

Abstract. **A time-dependent model of laser amplification in an Yb:YAG crystal is considered based on a system of balance equations, as well as radiation transfer and heat conduction equations. The model also takes into account the dependence of the laser characteristics of the gain medium on the injection wavelength and the effect of amplified spontaneous emission. This model is verified based on a diode-pumped amplifier with cryogenic cooling of active elements. The dependences of the gain on the pump pulse energy are experimentally measured for different amplification regimes and compared with simulation results.**

Keywords: *diode pumping, high pulse repetition rate, cryogenic temperatures, laser amplifier, heat conduction equation.*

1. Introduction

An important direction of modern studies in the field of laser physics is aimed at increasing pulse repetition rates (PRRs) in laser systems with high peak output powers. In recent years, a significant progress has been achieved in the development of light sources with subjoule energies and PRRs in the kilohertz range [1–4]. Such sources are used for generation of coherent X-ray radiation [5, 6] and laser acceleration of charged particles [7, 8]. High-energy ultrashort laser pulses are used for generation of extremely short pulses based on the OPCPA technology [9].

The main limiting factor in the development of laser systems with high PRRs is heating of the active elements of laser amplifier cascades [3, 10], which leads to phase distortions of the amplified radiation and to a decrease in the laser amplification efficiency. Active elements in cryogenically cooled systems experience considerable temperature gradients, which are responsible for the nonlinear dependence of the gain on the pump and cooling system parameters [11]. The narrow gain cross section spectrum of the Yb:YAG crystal (~1 nm at $T = 100$ K) in the laser transition region and its dependence on temperature make it necessary to adjust the amplifier operation regime to the amplified pulse parameters.

A source of CEP-stabilised pulses is being developed at the Institute of Laser Physics, Siberian Branch, Russian Academy of Sciences [12]. It includes a scalable solid-state laser system with a joule-level energy and a high PRR, which is used to pump a parametric amplifier. The key unit of this system is a two-cascade cryogenically cooled multidisk laser amplifier with a high-power diode pumping [13]. The active elements of this amplifier are diffusion-bonded YAG–Yb:YAG (10 at.% of Yb^{3+}) crystalline samples, which are pairwise attached to cryogenically cooled crystal holders from opposite sides. The samples have the form of a disk 25 mm in diameter with the thicknesses of the doped and undoped parts of 3.75 and 2 mm, respectively. The cooled face of the disk has a highly reflecting coating at the pump and gain wavelengths, which makes it possible to use the element as an active mirror. The amplifier contains eight active elements, which form two amplifier stages consisting of four elements each.

Injected pulses propagating in the amplifier make two round-trips first through the first and then through the second amplifier stage. The energy of injected pulses at the amplifier input is 10 mJ. The amplifier is pumped by eight pulsed diode lasers with a maximum power of up to 200 W each and a central wavelength of 940 nm. The active elements of the laser amplifier are cooled using closed-cycle Stirling cryostats. Such coolers improve the temperature stability of active elements, but their specific feature is that the heat sink temperature nonlinearly depends on the dissipated power.

2. Model

Previously [14], we have developed a three-dimensional time-dependent laser amplification model with allowance for the dependences of the thermophysical and laser characteristics of the active media on the temperature distribution [14]. The model takes into account the three-dimensional temperature distribution, temperature evolution with time, gain dynamics, relation of gain with heating, and temperature dependences of laser and thermophysical parameters, as well as the experimentally measured laser pump parameters and the depen-

G.V. Kuptsov, V.A. Petrov Institute of Laser Physics, Siberian Branch, Russian Academy of Sciences, prosp. Akad. Lavrent'eva 15B, 630090 Novosibirsk, Russia; Novosibirsk State Technical University, prosp. K. Marksa 20, 630073 Novosibirsk, Russia;
e-mail: kuptsov.gleb@gmail.com;
V.V. Petrov Institute of Laser Physics, Siberian Branch, Russian Academy of Sciences, prosp. Akad. Lavrent'eva 15B, 630090 Novosibirsk, Russia; Novosibirsk National Research State University, ul. Pirogova 2, 630090 Novosibirsk, Russia; Novosibirsk State Technical University, prosp. K. Marksa 20, 630073 Novosibirsk, Russia;
A.V. Laptev, A.V. Kirpichnikov, E.V. Pestryakov Institute of Laser Physics, Siberian Branch, Russian Academy of Sciences, prosp. Akad. Lavrent'eva 15B, 630090 Novosibirsk, Russia;
A.O. Konovalova Institute of Laser Physics, Siberian Branch, Russian Academy of Sciences, prosp. Akad. Lavrent'eva 15B, 630090 Novosibirsk, Russia; Novosibirsk National Research State University, ul. Pirogova 2, 630090 Novosibirsk, Russia

Received 18 June 2021
Kvantovaya Elektronika **51** (8) 679–682 (2021)
Translated by M.N. Basieva

dence of the heat sink temperature on the average pump power.

In the present work, we additionally take into account the dependence of the laser characteristics of the gain medium on the interacting wavelength and the effect of amplified spontaneous emission.

The temperature dependence of the full width of the luminescence cross-section profile σ_L at half maximum was obtained based on the experimental data published in [15] and approximated in the range of 80–300 K by the second-order polynomial

$$\Delta\sigma_L(T) = a + bT + cT^2, \quad (1)$$

where T is the temperature in kelvins and $a = 1.3$ cm, $b = -6.8 \times 10^{-3}$ cm K^{-1}, and $c = 8.6 \times 10^{-5}$ cm K^{-2} are the approximation coefficients.

The temperature dependence of the centre wavelength λ_{L0} of the luminescence cross section was determined based on the experimental data published in [16] and approximated in the range of 80–300 K by the first-order polynomial

$$\lambda_{L0}(T) = d + rT, \quad (2)$$

where $d = 1030.085 \times 10^{-7}$ cm and $r = 4.72 \times 10^{-10}$ cm K^{-1} are the approximation coefficients.

The luminescence cross section changes with temperature as [12]

$$\sigma_{L0}(T) = 0.75 + 1.77\exp(-[T - 273]/113.95). \quad (3)$$

Thus, the dependence of the luminescence cross section at the laser transition on temperature and wavelength has the form

$$\sigma_L(T, \lambda) = \sigma_{L0}(T)\exp(-4\ln 2[\lambda - \lambda_{L0}(T)]^2/\Delta\sigma_L^2(T)), \quad (4)$$

where λ is measured in centimetres.

The spectral width and amplitude of the absorption cross section spectrum at the pump wavelength for all temperatures considered in this paper are such that more than 98% of the pump radiation is absorbed in the doped layer (3.75 mm) of the element. Changes in the absorption cross section only slightly affect both the temperature distribution and the amplification process.

Another addition to the model was that we took into account the amplified spontaneous emission (ASE). In this case, according to Eqn (10) from [17], the gain implicitly depends on the pump beam diameter and the gain without allowance for the ASE. The equation is solved numerically, which leads to an increased computational load for calculating gains on large grids. To decrease the computational load in the case of a fixed pump beam radius, one can approximate small-signal gain with allowance for ASE γ_{ASE} for a given range of coefficients. In the present work, this approximation was performed for the pump beam diameter of 2 mm in the form

$$\gamma_{ASE}(\gamma_0) = A_0 + A_1\exp(-\gamma_0/t_1) + A_2\exp(-\gamma_0/t_2), \quad (5)$$

where γ_0 is the small-signal gain without allowance for the ASE and $A_1 = -15.46$ cm^{-1}, $t_1 = 66.1$ cm^{-1}, $A_2 = -5.53$ cm^{-1}, $t_2 = 8.87$ cm^{-1}, and $A_0 = 21.15$ cm^{-1} are the approximation coefficients.

Then, the transfer equation with allowance for the ASE is written as

$$\partial I_L/\partial z = cI_L\gamma_{AS}\{\sigma_L[nf_{11} - (n_t - n)f_{03}]\}, \quad (6)$$

where I_L is the amplified radiation intensity (W cm^{-2}), n_t is the concentration of dopant ions (cm^{-3}), n is the working level population density (cm^{-3}), f_{ji} reflects the population of the energy level E_{ji}, c is the speed of light (cm s^{-1}), and σ_L is measured in cm^2. The z direction corresponds to the pump beam axis.

3. Experiments

To verify the extended laser amplification model, we performed experiments on amplification of radiation with a broad spectrum.

A 2-mm diameter spot of pump radiation with a centre wavelength of 940 nm, a spectral width of ~10 nm, a peak power of 200 W was formed in the centre of the active element (AE). The injected radiation with a centre wavelength of 1029.8 nm and a pulse energy of 100 μJ was focused in the AE into a spot 1.9 mm in diameter and overlapped with the pump spot. The spatial distributions of the pump radiation and the radiation amplified in the AE are presented in Fig. 1.

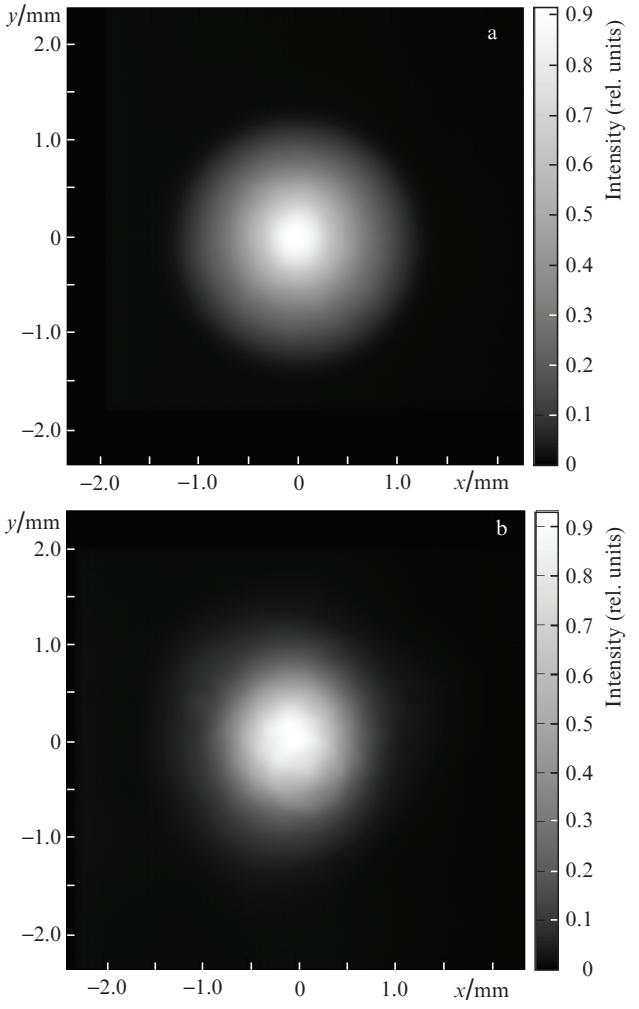

Figure 1. Spatial distributions of (a) pump and (b) amplified beams.

The injected beam was incident on the AE at an angle of 5.6° with respect to the normal. The full width at half maximum of the envelope of pulses in the time domain was ~500 ps. The spectral distribution of the amplified radiation is shown in Fig. 2.

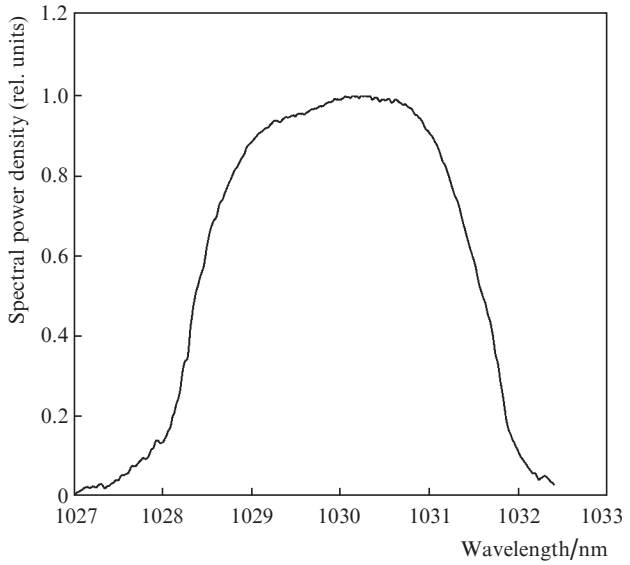

Figure 2. Spectral distribution of amplified radiation.

The injection and pump pulses were produced with identical repetition rates and synchronised in time. The experiment was controlled by a personal computer, and synchronisation was performed using a precision electronic module and controlled by photodiodes. The scheme of the experiment is shown in Fig. 3.

Experiments were performed for PRRs of 250, 500, and 1000 Hz. The measured dependences of the gain on the pump pulse energy for different PRRs are presented in Fig. 4. One can see that all curves have three characteristic regions, which are determined, first of all, by heating of the AE; these regions are characterised by a linear growth, a nonlinear growth, and a plateau. Heating of the AE in the region of the linear growth is insignificant and the average AE temperature lies in the range of 40–90 K, but only a part of the spectrum is amplified because, according to (1), the spectral width of the gain cross section becomes equal to the spectral width of the initial pulse only at a temperature of ~230 K. The nonlinear region is related to a stronger heating of the element, which leads to a decrease in the amplitude and simultaneously to an increase in the width of the luminescence cross section profile, as well as to an increase in the amplitude of the absorption cross section at the gain wavelength. Thus, the gain at the central wavelength decreases, but the injected pulse interacts with the AE in a wider wavelength range. In the last region, the effect of an increase in the spectral width is inferior to the effect of a decrease in the gain due to heating. An interesting consequence of this complex dependence is that, at an unchanged pump pulse energy, the gain increases with increasing PRR. This is explained by the fact that, at a fixed pump pulse energy, an increase in the PRR decreases the duty cycle, which leads to additional heating of the AE. An increase in the AE temperature causes broadening of the gain cross section spectrum, which is responsible for a higher gain at higher PRRs.

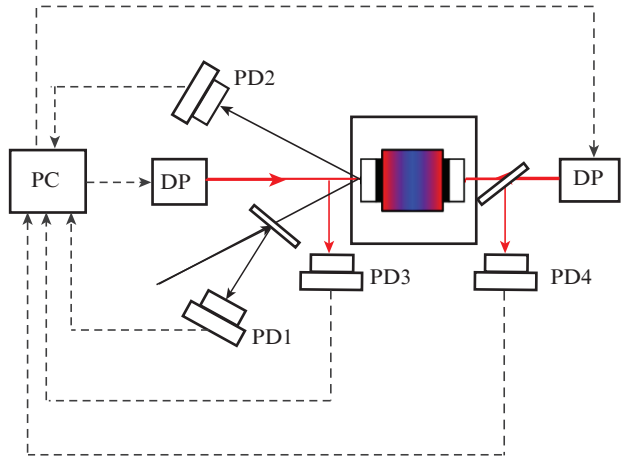

Figure 3. Experimental scheme for measuring the gain: (PC) personal computer; (DP) diode pumping modules; (PD1–PD4) photodiodes.

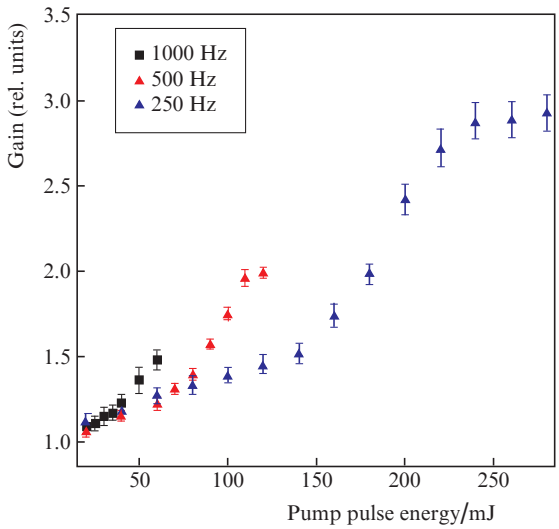

Figure 4. Dependences of the gain on the pump pulse energy for PRRs of 250, 500, and 1000 Hz.

The maximum pump pulse duration for a given PRR in the experiment was determined by the maximum permissible power dissipated by the cooling system.

It is necessary to note that the regions of both linear and nonlinear growth have almost identical slopes independently of the PRR. This occurs because heating of the element depends only on the average pump power. In our experiments, the pump pulse duration did not exceed 1.4 ms and the characteristic time estimated by the Fourier number was on the order of 0.1 s, because of which direct local heating of the AE during pumping did not considerably affect the amplification process.

The maximum gain in all experiments was achieved when the pump and injected pulses were shifted in time so that the injection pulse was incident on the AE at the instant of the pump pulse termination.

Taking into account the experimentally measured parameters, we numerically simulated the gain based on the extended model of laser amplification. The simulation results are presented in Fig. 5.

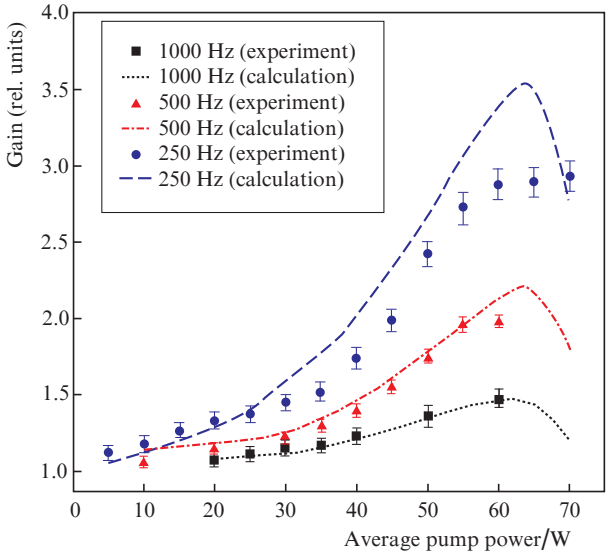

Figure 5. Results of simulation of the dependence of the gain on the average pump power in comparison with experimental data for PRRs of 250, 500, and 1000 Hz.

The allowance for the dependences of the laser characteristics of the gain medium on the injection wavelength and the AE temperature considerably affects the simulation results. Ignorance of these dependences leads to an increase in the calculated gain (by up to five times). With decreasing PRR and increasing pump pulse energy, the ASE begins to exert a considerable effect. In particular, the allowance of this effect at a PRR of 1000 Hz leads to a decrease in the gain on average by 6%, but this decrease at 500 Hz is already ~40%, and the allowance for the ASE at a PRR of 250 HZ causes a threefold decrease in the gain. The simulation results agree well with the experimental data. The dependences of the gain on the average pump power shown in Fig. 5 clearly show that the linear, nonlinear, and constant regions of the curves depend only on the average pump power and their boundaries are determined by the thermophysical parameters of the AEs and the cooling system.

4. Conclusions

The time-independent three-dimensional model of laser amplification with allowance for the dependences of the thermophysical and laser characteristics of active media on the temperature distribution was extended by taking into account the dependence of the laser characteristics of the gain medium on the injection wavelength and by partial allowance for the ASE effect.

The process of laser pulse amplification in an Yb:YAG active element with high temperature gradients was simulated taking into account the experimentally measured parameters of a multidisk laser amplifier. The extended model was verified by experiments on amplification of radiation with a broad spectrum. The simulation data agree well with the experimental results, which confirms the correctness of the extended model of laser amplification.

The results of the study make it possible to optimize the amplifier parameters at cryogenic temperatures to achieve maximum powers of amplified pulses with a given repetition rate.

Acknowledgements. This work was supported by the Russian Foundation for Basic Research (Grant No. 20-02-00529-a), the Russian Foundation for Basic Research and Novosibirsk oblast government (Grant No. 19-42-543007), and the Ministry of Science and Higher Education of the Russian Federation (Grant No. 121033100057-1).

References

1. Wang Y., Chi H., Baumgarten C., Dehne K., Meadows A.R., Davenport A., Murray G., Reagan B.A., Menoni C.S., Rocca J.J. *Opt. Lett*., **45**, 6615 (2020).
2. Nubbemeyer T., Kaumanns M., Ueffing M., Gorjan M., Alismail A., Fattahi H., Brons J., Pronin O., Barros H.G., Major Z., Metzger T., Sutter D., Krausz F. *Opt. Lett*., **42**, 1381 (2017).
3. Baumgarten C., Pedicone M., Bravo H., Wang H., Yin L., Menoni C.S., Rocca J.J., Reagan B.A. *Opt. Lett*., **41**, 3339 (2016).
4. Herkommer C., Krötz P., Jung R., Klingebiel S., Wandt C., Bessing R., Walch P., Produit T., Michel K., Bauer D., Kienberger R., Metzger T. *Opt. Express*, **28**, 30164 (2020).
5. Reagan B.A., Berrill M., Wernsing K.A., Baumgarten C., Woolston M., Rocca J.J. *Phys. Rev. A*, **89**, 053820 (2014).
6. Depresseux A., Oliva E., Gautier J., Tissandier F., Nejdl J., Kozlova M., Maynard G., Goddet J.P., Tafzi A., Lifschitz A., Kim H.T., Jacquemot S., Malka V., Ta Phuoc K., Thaury C., Rousseau P., Iaquaniello G., Lefrou T., Flacco A., Vodungbo B., Lambert G., Rousse A., Zeitoun P., Sebban S. *Nat. Photonics*, **9**, 817 (2015).
7. Salehi F., Goers A.J., Hine G.A., Feder L., Kuk D., Miao B., Woodbury D., Kim K.Y., Milchberg H.M. *Opt. Lett*., **42**, 215 (2017).
8. Morrison J.T., Feister S., Frische K.D., Austin D.R., Ngirmang G.K., Murphy N.R., Orban C., Chowdhury E.A., Roquemore W.M. *New J. Phys*., **20**, 022001 (2018).
9. Divoky M., Smrz M., Chyla M., Sikocinski P., Severova P., Novak O., Huynh J., Nagisetty S.S., Miura T., Pilař J., Slezak O., Sawicka M., Jambunathan V., Vanda J., Endo A., Lucianetti A., Rostohar D., Mason P.D., Phillips P.J., Ertel K., Banerjee S., Hernandez-Gomez C., Collier J.L., Mocek T. *High Power Laser Sci. Eng*., **2**, e14 (2014).
10. Tamer I., Keppler S., Hornung M., Korner J., Hein J., Kaluza M.C. *Laser Photonics Rev*., **12**, 1700211 (2018).
11. Petrov V.V., Kuptsov G.V., Nozdrina A.I., Petrov V.A., Laptev A.V., Kirpichnikov A.V., Pestryakov E.V. *Quantum Electron*., **49** (4), 358 (2019) [*Kvantovaya Elektron*., **49** (4), 358 (2019)].
12. Kuptsov G.V., Petrov V.A., Petrov V.V., Laptev A.V., Kirpichnikov A.V., Pestryakov E.V. *Proc. SPIE*, **11322**, 113220V (2019).
13. Petrov V.V., Kuptsov G.V., Petrov V.A., Laptev A.V., Kirpichnikov A.V., Pestryakov E.V. *Quantum Electron*., **48** (4), 358 (2018) [*Kvantovaya Elektron*., **48** (4), 358 (2018)].
14. Petrov V.V., Petrov V.A., Kuptsov G.V., Laptev A.V., Kirpichnikov A.V., Pestryakov E.V. *Quantum Electron*., **50** (4), 315 (2020) [*Kvantovaya Elektron*., **50** (4), 315 (2020)].
15. Dong J., Bass M., Mao Y., Deng P., Gan F. *J. Opt. Soc. Am. B*, **20** (9), 1975 (2003).
16. Petrov V.A., Petrov V.V., Kuptsov G.V., Laptev A.V., Galutskiy V.V., Stroganova E.V. *Laser Phys*., **31**, 035003 (2021).
17. Vadimova O.L., Mukhin I.B., Kuznetsov I.I., Palashov O.V., Perevezentsev E.A., Khazanov E.A. *Quantum Electron*., **43** (3), 201 (2013) [*Kvantovaya Elektron*., **43** (3), 201 (2013)].